Bio-synthesized iron oxide nanoparticles for cancer treatment

Edouard Alphandéry

BIO-SYNTHESIZED IRON OXIDE NANOPARTICLES FOR CANCER TREATMENT

Edouard Alphandéry[+,++,+++]

[+]Paris Sorbonne Université, Muséum National d'Histoire Naturelle, UMR CNRS 7590, IRD, Institut de Minéralogie, de Physique des Matériaux et de Cosmochimie, IMPMC, 75005 Paris, France

[++]Nanobacterie SARL, 36 boulevard Flandrin, 75116, Paris, France.

[+++]Institute of Anatomy, UZH University of Zurich, Instiute of Anatomy, Winterthurerstrasse 190, CH-8057, Zurich, Switzerland.

Email address: edouardalphandery@hotmail.com, phone: 0033632697020

ABSTRACT: Various living organisms, such as bacteria, plants, and animals can synthesize iron oxide nanoparticles (IONP). The mechanism of nanoparticle (NP) formation is usually described as relying on the reduction of ferric/ferrous iron ions into crystallized nanoparticulate iron that is surrounded by an organic stabilizing layer. The properties of these NP are characterized by a composition made of different types of iron oxide whose most stable and purest one is maghemite, by a size comprised between 5 and 380 nm, by a crystalline core, by a surface charge which depends on the nature of the material coating the iron oxide, and by certain other properties such as a sterility, stability, production in mass, absence of aggregation, that have only been studied in details for IONP synthesized by magnetotactic bacteria, called magnetosomes. In the majority of studies, bio-synthesized IONP are described as being biocompatible and as not inducing cytotoxicity towards healthy cells. Anti-tumor activity of bio-synthesized IONP has mainly been demonstrated *in vitro*, where this type of NP displayed cytotoxicity towards certain tumor cells, *e.g.* through the anti-tumor activity of IONP coating or through IONP anti-oxidizing property. Concerning *in vivo* anti-tumor activity, it was essentially highlighted for magnetosomes administered in different types of glioblastoma tumors (U87-Luc and GL-261), which were exposed to a series of alternating magnetic field applications, resulting in mild hyperthermia treatments at 41-45 °C, leading to the full tumor disappearance without any observable side effects.

KEYWORDS: magnetosomes, cancer, natural iron oxide nanoparticle, alternating magnetic field, magnetic hyperthermia, nano-oncology, glioblastoma, GBM, anti-tumor activity, nanomedicine, nanoparticle, magnetotactic bacteria.

ABREVIATIONS:

AMF: Alternating magnetic field;

DNP: Duration of nanoparticle production;

IONP: Iron oxide nanoparticles;

MC: Chains of magnetosomes extracted from AMB-1 magnetotactic bacteria;

MHT: Magnetic hyperthermia;

MTB: Magnetotactic bacteria;

MS: Magnetic session, time during which an AMF is applied on NP;

M-PLL: Iron oxide magnetosome minerals coated with poly-L-lysine;

NPY: Nanoparticle production yield;

NaOH: Sodium hydroxide;

NP: Nanoparticles;

GBM: Glioblastoma multiform;

UV: ultra-violet;

BNF: A type of chemically synthesized nanoparticles that was purchased from the company Micromod;

TEM: Transmission electron microscopy;

INTRODUCTION

Nanoparticles (NP) have raised a surge of interest in the field of cancer, leading to the development of various technologies, such as the irradiation of NP located in tumors by X-rays, (1), the specific delivery or targeting of drugs in the tumor using drugs associated with IONP, (2), the heating of nanoparticles under the application of an alternating magnetic field to eradicate a tumor through localized moderate heating, (3). Among the different types of nanoparticles, iron oxide nanoparticles (IONP) are particularly attractive because of their biocompatibility and their proven efficacy for the treatment of iron anemia diseases, (2), and cancer using magnetic hyperthermia (MHT), (3, 4). However, the majority of chemical syntheses use toxic products, (5), which may end up as trace elements in the final IONP formulation. To overcome this hurdle, it has recently been proposed to use natural manufacturing methods to bio-synthesize IONP, using certain organisms such as bacteria, (6), plants, (7), yeast, fungi, (8), seaweeds, (9), or some of their enzymes or proteins, which often play a central role in the reduction of ferrous/ferric iron ions into crystallized nano-particulate iron, (10, 11, 12, 13, 14)., This article reviews the different modes of IONP bio-synthesis, the physicochemical properties, the bio-compatibility, as well as the anti-tumor properties of these IONP. Magnetosomes, which are synthesized by magnetotactic bacteria (MTB), appear to be at the most advanced stage of development among the different types of bio-synthesized IONP, allowing foreseeing their use as anti-cancer agents. Indeed, a magnetosome manufacturing method has been developed, which relies on the following well-established steps: i) amplification of MTB, ii) extraction of magnetosomes from MTB, purification of magnetosome minerals to remove organic/pyrogenic/immunogenic material, and iii) stabilization of these purified minerals with different synthetic coatings. This process yields magnetosomes with properties that are compatible with their use for cancer treatment, *i.e.*: i) a sufficient nanoparticle production yield (NPY), *i.e.* NPY ~ 10 mg of magnetosomes per liter of growth medium, (15), ii) a very high purity, *i.e.* these magnetosomes are composed of 99.8% of iron relatively to other metals, (15) iii) a very good crystallinity, iv) a stable composition of maghemite, (16), v) an arrangement in chains, (17, 18), and v) a sterility or non-

pyrogenicity, (17, 18). Furthermore, magnetosomes were shown to display excellent anti-tumor activity when they were administered in intracranial U87-Luc human GBM tumors or in subcutaneous GL-261 murine GBM tumors and exposed to several sessions of application of an alternating magnetic field, leading to the complete disappearance of these tumors, (19, 20, 21).

I. Different methods of iron oxide nanoparticle bio-synthesis.

IONP can first be synthesized intracellularly by specific bacteria, which are called magnetotactic bacteria (MTB). For that, MTB cytoplasmic membrane is invaginated, resulting in the formation of intracellular vesicles in which extracellular ferric/ferrous iron ions have diffused, further leading to the nucleation of magnetite crystals, called magnetosomes. The whole process of magnetosome formation is controlled by specific mam (magnetosome membrane) or mms (magnetic particle membrane specific) genes and their associated proteins, (22). Magnetosomes, which are well-crystallized mono-domain crystals with ferrimagnetic magnetic properties and an arrangement in chains inside MTB, yield an efficient coupling between their magnetic moment and the external earth magnetic field, hence enabling MTB to swim in the direction of the earth magnetic field, through a mechanism called magnetotaxis. Most MTB can't be used for biotechnological applications, either because their growth conditions are not well established or because they produce a too small quantity of magnetosomes. To the author knowledge, only one species of MTB, which is called MSR-1 *Magnetospirillum gryphiswaldense*, can produce magnetosomes in large quantities, *i.e.* ~ 10 mg/liter, using a two steps method in which MTB are first pre-amplified in an iron depleted growth medium and are then grown in iron-rich conditions to produce magnetosomes in mass, (15). Furthermore, a recent study has shown the possibility to follow this two steps method using minimal growth media not containing any toxic products such as CMR chemicals, heavy metals, or products originating from microorganisms (yeast extracts), paving the way towards the use of MSR-1 MTB for biotechnological applications, (15). Secondly, IONP can be synthesized outside of certain types of bacteria such as *Geobacter sulfurreducens* or actinomycetes MS-2, (23). A typical protocol consists in growing these bacteria during several days and then adding to the bacterial suspension or its supernate a source of iron III, which is further reduced into iron II, resulting in the formation of nano-minerals of various phases, *i.e.* essentially magnetite, goethite, hematite, siderite or vivianite. In this case, the mechanisms of nanoparticle formation most probably involve specific enzymes localized outside of these bacteria, which are responsible for the reduction reactions, although such mechanisms are not described in details in the literature, (23, 24, 25). Thirdly, IONP bacterial synthesis can also occur at the surface of

certain bacteria such as *K. oxytoca* or *Staphylococcus warneri*, which synthesize biogenic polysaccharide-iron hydrogel nanoparticles, known as Fe (III)-exopolysaccharide (Fe-EPS) through the reduction of ferric citrate under anaerobic conditions, (26, 27). Fourthly, specific parts of bacteria such as their flagella can be used for nanoparticle synthesis. Specific flagella filaments have indeed been produced through genetic manipulations of Salmonella bacteria, which contain binding sites of iron/magnetite, where nano-minerals can form. These minerals partially cover the filamentous biological template and align in one-dimensional magnetic nanostructures, (28).

Besides bacteria, plant extracts, *i.e.* essentially leaves and seeds, can be used to bio-synthesize IONP. The first step of this synthesis consists in isolating and heating the various extracts, *e.g.* leave extracts of *Skimma laureola*, *Rosmarinus officinalis*, *eucaliptus*, *Sida cordifolia*, *green tea*, *Garlic Vine*, *C. sativum*, *M. oleifera*, or seed extracts of *Fenugreek* or *Psoralea corylifolia*. These extracts are usually heated, filtered to eliminate impurities, and then mixed with various iron sources such as $FeCl_3$, $Fe(NO_3)$, $FeSO_4$, $FeCl_2$, using different ratio between the volume of extracts and that of iron sources. It results in the reduction of iron ions into nanoparticles composed of iron or iron oxide, *e.g.* Fe_2O_3 and Fe_3O_4. In some cases, this mixture is carried out in the presence of a chemical such as ammonia and/or by sonication to promote the reduction reaction. The suspension thus obtained is then usually centrifuged and washed with alcohol or water to separate organic residues from the nanoparticles (29-39).

Certain by-products of animal species, such a albumen extracts, can be heated and mixed in the presence of NaOH and ammonia with an iron source, *i.e.* $Fe(NO_3)$, and then auto-claved at 150–220°C for 4–10 hours to produce IONP, (40).

Other IONP fabrication processes involve a mixture of biological and non-biological methods. For example, it was reported that ferrous ions can be oxidized by *Acidithiobacillus ferrooxidans* bacteria under acid conditions into Fe^{3+}, and these ions can then further be precipitated into $Fe(OH)_3$ in the presence of ammonia, and this precipitate can be calcinated in muffle furnace to yield Fe_2O_3 nanoparticles, (41).

Lastly, mechanisms of IONP fabrication by living organisms can be mimicked using engineering processes. For example, amphiphilic block co-polymers can be self-assembled into vesicles, called

polymersomes, to mimic liposomes. These vesicles are made of 2 di-block co-polymers of 246 ± 137 nm in size, made of PEG113-PHPMA400 that makes the vesicles furtive due to the presence of PEG and PMPC28-PHPMA400 that provides acidic iron binding carboxylates, which are used for IONP nucleation. In this case, IONP formation is carried out by electroporation of these vesicles in the presence of an iron solution, which triggers iron diffusion inside the vesicles, and is followed by iron crystallization to form nanoparticles, (42). In a second example, specific proteins displaying active loops involved in iron biomineralization, *i.e.* Mms13 and MmsF, were used produce IONP, (43). In a third example, a 14-mer bi-functional copolypeptide was used in combination with ginger extracts to bio-mineralize iron into magnetite, (44).

II. Properties of bio-synthesized iron oxide nanoparticles.

Bio-synthesized IONP have been reported to be of various compositions including ferrihydrite $(Fe^{3+})_2O_3 \bullet 0.5H_2O$, goethite ($\alpha FeO(OH)$), hemathite ($\alpha Fe_2O_3$), siderite ($FeCO_3$), lepidocrocite $\gamma FeO(OH)$, maghemite (γFe_2O_3), and magnetite (Fe_3O_4). IONP compositions can either be made of mixed iron oxide phases, *e.g.* IONP synthesized by *G. sulfurreducens* bacteria are composed of magnetite, goethite, hematite, and siderite, or of a single iron oxide phase, *e.g.* magnetite for magnetosomes contained inside MTB and mostly maghemite for magnetosomes extracted from MTB, (45). Concerning IONP multi-phase composition, it is usually not specified whether it corresponds to different phases within each individual nanoparticle or to different mono-phases within the assembly of nanoparticles. It is therefore difficult to conclude if such composition is that of individual nanoparticles or of an assembly of nanoparticles taken as a whole. Although IONP are in some cases reported to be composed of one type of iron oxide, it does not necessarily mean that another phase is not present. One of the main interests of the iron oxide composition comes from the specific magnetic properties that it can confer to nanoparticles. To the other knowledge, among the different phases, only NP made of maghemite or magnetite have achieved a non-zero remnant magnetization at physiological temperature, *i.e.* the presence of a non-zero magnetization in the absence of application of an external magnetic field, under certain conditions in terms of NP sizes, which need to be larger than typically ~10-20 nm, and NP crystallinity, which should be of sufficient

quality to enable the formation of a stable magnetic moment within the NP. Such property notably enables reaching improved heating properties in a MHT treatment. It should be noted that very few biological syntheses achieve such properties, which have to the author knowledge only truly been reported for magnetosomes. Furthermore, while magnetite easily oxidizes into maghemite, *i.e.* even if IONP are maintained in an anoxic environment before their administration to prevent them from oxidizing they will certainly oxidize into maghemite *in vivo*, maghemite is very stable and should not oxidize at physiological temperatures. Because of its higher stability, the maghemite composition is probably preferable to the magnetite one for injections in humans.

Size is another essential parameter that defines IONP properties, whose value lies between 5 and 380 nm for the analyzed IONP (table 1). In principle, smaller nanoparticles have a ratio between their exposed surface and internal volume, which is larger than that of larger NP, and therefore potentially also a higher reactivity at their surface. However, size is a complex notion, which depends on several parameters such as: i) the method used for its measurement, *i.e.* DLS usually results in the measurement of NP of larger sizes than TEM, ii) the type of nanoparticle considered, *i.e.* with or without a coating, iii) NP organization, *i.e.* strongly interacting NP may be very close to each other leading to the size of a single NP equal to that of a NP assembly. For these reasons, it is not straightforward to compare NP sizes resulting from various IONP bio-syntheses.

In general, as it is the case for NP size, NP crystallinity can be controlled or adjusted either directly by the living organism synthesizing IONP such as MTB, (22), or indirectly through the adjustment of certain parameters such as the temperature or pH of the reduction reaction of ferrous/ferric ions into crystallized IONP, (23, 24, 25). Whereas most IONP were reported to be crystalline, some of them were also described as being amorphous (table 1). Most NP are probably neither totally crystalline nor totally amorphous. However, to be sure of that, one would need to use as a reference a scale that measures the level of NP crystallinity, which could be defined in a standard and notably take into account the presence (or not) of vacancies, crystalline defaults, alignment or misalignments of crystallographic planes in IONP. To date, such standard does not exist and the notion of crystallinity applied to IONP is therefore prone to different

interpretations. Most of time, it would be assumed that IONP observable under electron microscopy with a solid well-defined nano-metric shape and possibly crystallographic planes would be crystalline, but NP crystallinity remains a largely undefined notion.

With regard to NP surface charge, which is often described as playing an essential role in IONP anti-tumor activity, (46), notably due to IONP cellular internalization properties, which depend on the value of this parameter, (47, 48), the following specificities associated with IONP bio-synthesis should be underlined. In a first case, bio-synthesized IONP are surrounded by a natural membrane that originates from the organism synthetizing them, and the nature of this material then determines the value of IONP surface charge. In a second case, the original organic membrane surrounding IONP is removed and replaced by a synthetic coating. To the author knowledge, this second approach was only followed with magnetosomes, which were purified to remove most organic materials originating from MTB, and naked magnetosome minerals were then coated with various compounds that yielded either a positive surface charge at physiological pH for poly-L-lysine, poly-ethylene-imine, and chitosan, or a negative surface charge at this pH for carboxy-methyl-dextran, oleic acid, neridronate, and citric acid, (17, 18). In a biotechnological manufacturing process, this second approach seems more appropriate than the first one since it enables adjusting the surface charge by accurately choosing NP coating material.

To be injectable to humans, IONP should be sufficiently stable. In biotechnology, one can distinguish two types of stability, which are firstly the stability during NP administration, *i.e.* IONP should remain dispersed with a sufficient homogeneity to be injectable in an organism, and secondly the long term stability, *i.e.* IONP should not degrade or lose their activity during a certain time period of typically a few months so that they can be used when needed within this lapse of time. In most studies, bio-synthesized IONP were reported to be stable, but it was not specified whether this stability corresponded to a short or long term one, and in which conditions it was measured, *i.e.* in which medium and with which method or equipment. When one describes IONP stability, one should also distinguish the stability of the iron oxide core, which is probably higher for crystalline than amorphous structures although this has not yet been determined experimentally for bio-synthesized IONP, from the stability of the coating. The coating is

most of the time assumed to be the main source of IONP instability, probably because of its non-crystalline structure or exposure to the surrounding medium, which can be degrading, *e.g.* through oxidation. IONP stability is therefore mainly deduced from the stability of its coating. The natural organic coating, which is made of various biomolecules, phytochemicals, components of leaf or plant extracts, bacterial debris, proteins, lipids (table 1), may stabilize IONP and prevent the aggregation/sedimentation of these nanoparticles. However, it will certainly degrade over time and stability studies should examine the mechanism of degradation of this coating and possibly determine the conditions under which it does not occur. To the author knowledge, detailed stability studies of bio-synthesized IONP were only carried out for coated magnetosome minerals, for which it was estabilished that a suspension containing such minerals mixed in water remain stable up to 100 mg/mL during a few minutes, a time that is sufficiently long to enable their intra-tumor injection. It was also shown that these particles could be kept in the fridge for a few months without degrading.

Sterility is another required property of a biotechnological product to enable its administration to a human. In most studies, sterility of bio-synthesized IONP is neither sought for nor assessed. Unsterile conditions of IONP fabrication are presented, which implies that IONP resulting from these processes would need to be sterilized after their synthesis. To the author knowledge, the only bio-synthesis that yielded sterile IONP was achieved with the magnetosomes by purifying magnetosome minerals originating from MTB using chemical treatments, *i.e.* by mixing magnetosomes with detergents, or physical methods, i.e. through magnetosome heating. Using these processes, it was shown that the LPS concentrations could be reduced from 2000-12000 EU/mL/mgFe for chains of magnetosomes extracted from MTB without further treatment in suspension down to 10-200 EU/mL/mgFe for treated coated magnetosome minerals, (18), hence falling within the range of endotoxin concentrations that is acceptable in a biotechnological product and shall prevent sceptic shocks on humans, (18).

With regard to immuno-genicity, the administration of magnetosomes in mouse tumors followed by the application of an alternating field triggered a certain level of immune response, which was highlighted by the presence of poly-nuclear neutrophiles in the injection region, (19).

Other aspects, which need to be addressed to enable IONP human injection but are rarely mentioned, include: i) the type of surfactant/adjuvant used for mixing IONP for injection, *i.e.* apparently only magnetosomes were shown to be dispersible in water at high concentrations of up to typically ~100 mg/mL, ii) the level of purity of bio-synthesized IONP, *i.e.* it seems that only maghemite and magnetite could reach a very pure iron oxide composition of more than 99.8% in iron compared with other metals, where such high level of purity was only reported for magnetosomes, (15), iii) IONP organization that can have an impact on IONP stability/bio-distribution/cellular internalization, which was only studied in details under different conditions for magnetosomes that organize in chains, hence favoring an homogenous distribution of these particles by preventing their aggregation, (49), iv) the absence or presence of specific activity of IONP coating, *e.g.* it was suggested that a coating made of leaf extracts of plants *Albizia adianthifolia* was able to capture free radicals and yield anti-oxidation properties, (50).

Lastly, the nanoparticle production yield (NPY) should be sufficiently large to enable the treatment of a large enough number of patients suffering from cancer. Although this parameter is very important, it is almost never mentioned in the literature. Maybe, this is due to the lack of a clear definition. Indeed, defining NPY as being simply the quantity of nanoparticles produced per litter or unit volume of IONP production is incomplete. To be more accurate, NPY should also take into account: i) the duration of nanoparticle production (DNP), *i.e.* one could define NPY/DNP instead of NPY, ii) the step at which NPY is measured, *i.e.* NPY should preferably be measured when IONP are in their final formulation form where they are ready for injection and possibly also at some earlier steps of the fabrication process, iii) the type of element chosen to measure IONP concentration, *i.e.* in case of IONP one could estimate IONP concentration from its iron content assuming that IONP activity mainly comes from iron, iv) IONP fabrication process whose parameters such as pH, temperature, concentration of biological extracts, ratio between the quantity of iron source and quantity of reducing agents, should preferably be optimized. Furthermore, the optimization of NPY should lead to a process that reaches a relatively large IONP production while being compatible with medical regulations. Furthermore, although this point is rarely discussed in the literature large values of NDPY and NDPY/DNP parameters are in principle only

necessary for IONP, which are stable over short periods of times, necessitating the rapid production of the IONP therapeutic dose. In case of very stable IONP, which can be stored for long periods of time without losing their therapeutic activity, lower values of NDPY and NDPY/DNP could be acceptable. To the author knowledge, magnetosomes are the only bio-synthesized IONP for which NPY of ~10 mg per liter of growth medium and NPY/DNP of ~1 mg per liter per day, have been estimated, using growth media that are compatible with a biotechnological production, *i.e.* without CMR chemicals, products originating from microorganisms (yeast extracts), and heavy metals. As mentioned above, to assess whether the NPY is sufficient, it should be compared with the therapeutic dose necessary to treat one patient. Given that such a dose is ~0.1 gram of IONP per patient, approximately 10 liters of cultures would be sufficient to treat one patient.

III. Biocompatibility of bio-synthesized iron oxide nanoparticles.

In general, IONP are considered bio-compatible, (2). However, the majority of chemical synthesis relies on the use of toxic chemicals such as hydrazine or potassium bi-tartrate that can end up as trace elements in the final nanoparticle formulation. By using a biological synthesis, it is possible to synthesize IONP without the use of toxic products. For example, a recent study reported the growth of magnetotactic bacteria in the absence of any CMR products, yeast extracts, or heavy metals, using a method that is compatible with pharmaceutical standards, (15). Another interesting factor, which is often mentioned in the literature and can prevent nanoparticle toxicity, is the biocompatible coating, *e.g.* made of phytochemicals, that naturally surrounds IONP following nanoparticle synthesis by a living organism, (51, 52, 53, 54). Although it is certainly true that the presence of such coating can improve nanoparticle bio-compatibility, it is not obvious to keep it in a biotechnological process since such coating would be difficult to fully characterize, to obtain reproducibly with the exact same composition, and to sterilize without inducing its destruction. This is the reason why an alternative method of preparation has been suggested with the magnetosomes, which consists in removing the organic coating produced by magnetotactic bacteria, which is made of biological material such as proteins and lipids, and in replacing

it by a synthetic coating that can more easily be characterized, (17, 18). Regarding the bio-compatibility of these bio-synthesized IONP, it has been highlighted through the following results: i) an absence or weak cytotoxicity, *i.e.* a cytotoxicity associated with a percentage of cellular inhibition lower than 30%, towards different healthy cells such as 3T3 fibroblast cells up to 15 µg/mL of IONP (55), Neuro2A and HUVEC brain cells up to 150 µg/mL of IONP (56), human red blood cells and macrophages up to 15 µg/mL of IONP (57), or embryonic kidney HEK-293 cells up to 500 µg/mL of IONP (37), ii) no toxicity towards embryos of zebra-fish for a IONP concentration lower than 5 mg per liter (58), iii) no significant toxicity towards a number of aquatic organisms such as cyanobacteria, alga, and invertebrate organisms (59), iv) no acute toxicity up to 2000 mg of IONP per kg of mouse body weight when IONP are given orally to mice (60). Most interestingly, it was shown that bio-synthesized IONP were less toxic towards various organisms than amorphous complexes of free iron ions, (35), suggesting that the specific nanoparticulate formulation can prevent iron toxicity or reduce it compared with that of free iron ions. In some studies, the toxicity of bio-synthesized IONP was compared with that of chemically synthesized IONP. For example, it was shown that IONP formed through the reduction of metal ions using aqueous sorghum bran extracts was rapid and resulted in water-soluble, biodegradable IONP coated with phenolic compounds, which were less toxic than IONP prepared using conventional $NaBH_4$ reduction protocols, (61).

IV. Anti-tumor efficacy of bio-synthesized iron oxide nanoparticles.

IV.I. *In-vitro* anti-tumor activity

Anti-tumor activity of bio-synthesized IONP was essentially highlighted using *in vitro* cytotoxicity assessment, where it was shown that such nanoparticles could inhibit the growth of several types of tumor cells including leukemia (Jurkat cells), breast cancer (MCF-7 cells), cervical cancer (HeLa cells), and liver cancer (HepG2 cells), (39, 62). To explain this efficacy, some studies have brought forward the role of the natural IONP coating, *e.g.* a coating made of rosemary extracts containing polyphenols yielding anticancer effects, which inhibited the growth of 4T1 breast cells with a larger inhibition for the plant extracts associated to IONP, *i.e.* $IC_{50} \sim 44$ µg/mL, than for the extracts alone, *i.e.* $IC_{50} \sim 100$ µg/ml, (37).

Other studies have reported that IONP toxicity towards human breast AMJ-13 and MCF-7 cancer cells, could be due to IONP acting as free radical scavengers, yielding anti-oxidant effects, and cellular death through apoptosis, (50). For some of these nanoparticles, a relative absence of cytotoxicity towards both tumor and healthy cell lines has been observed for nanoparticle concentration lower than 1 mg/mL (24, 63).

V.II. *In vivo* antitumor activity

Few studies have reported *in vivo* anti-tumor activity of bio-synthesized IONP. To the author knowledge, only magnetosomes were tested to this effect, using two types of suspensions, containing either pyrogenic chains of magnetosomes directly extracted from MTB without further treatment (CM) or purified non-pyrogenic iron oxide magnetosome minerals stabilized by a ploy-L-lysine coating (M-PLL). Two types of GBM tumors were treated, *i.e.* subcutaneous murine GBM GL-261 tumors of ~ 100 mm^3 or intracranial human GBM U87-Luc tumors of 2 mm^3. The protocol of treatment consisted in administering intra-tumorally, through one or two administration(s), 13 µg of CM or 500-700 µg of M-PLL per mm^3 of U87-Luc tumors or 25-50 µg of M-PLL per mm^3 of GL-261 tumor, followed by 15 to 27 sessions of 30 minutes of application of an alternating magnetic field (AMF) of 30 mT and 198 kHz (table 2). Temperature increases reached during the various treatment sessions, which are summarized in table 3, occurred within a much more important number of sessions for M-PLL than for BNF-starch. Figure 1 illustrates how the treatment of intracranial and subcutaneous GBM tumors was carried out by using M-PLL (Figure 1(c)), which originated from chains of magnetosomes (Figure 1(b) and whole MTB (Figure 1(a)), were administered in subcutaneous GL-261 tumors and intracranial U87-Luc tumors, and excited through various applications of an alternating magnetic field, which resulted in full tumor disappearance (Figures 1(d) and 1(e)).

The most striking results of these treatments are characterized by (table 2):

- The full tumor disappearance obtained using a low quantity of CMM (13 µg/mm^3) among a significant percentage of treated mice of 40% (19);

- Tumor eradication among 100% of treated mice reached by increasing the quantity of magnetosomes from 13 µg/mm3 to 400-800 µg/mm^3 (20);
- An anti-tumor efficacy that was more pronounced for M-PLL than for magnetosome chemical counterparts (BNF-Starch), even so BNF-Starch were re-administered in the tumor a larger number of times than M-PLL, (4 and 6 mice re-injected for M-PLL and BNF, respectively), and the AMF strength applied during the first session was higher for BNF (26.5 mT) than for M-PLL (20 mT), table 4, (21), to attempt reaching similar heating temperatures for both types of nanoparticles;

To explain the superior anti-tumor activity of bio-synthesized IONP formulations compared with their chemical counterparts, the following explanations, which are summarized in Figure 2, have been brought forward. Firstly, due to their large size, good crystallinity, and magnetic mono-domain ferrimagnetic behaviors, magnetosomes display excellent heating properties when they are exposed to an alternating magnetic field, (53), yielding SAR values that can exceed 1000 W/gFe using AMF of moderately high strength and frequency of 20 mT and 200 kHz. These SAR values are higher than those usually reported for chemically synthesized nanoparticles, (64). Secondly, magnetosomes have been shown to internalize in various cells, where this faculty is enhanced under the application of an alternating magnetic field , (49), potentially enabling them to release an anti-tumor drugs intra-cellularly such as LPS associated with CM, (19). Thirdly, tissue biodistribution studies have shown that magnetosomes can form dense assembly of nanoparticles localized in the tumor region that can help magnetosomes to remain in the tumor during several treatment sessions, hence resulting in magnetosome tumor bio-persistence. Fourthly, cellular death induced by magnetosome treatment has been shown to mainly occur through apoptosis, most probably due to the moderate heating temperatures of 41-45 °C reached during treatment. This is an important aspect since tumor cells often lose their faculty to dye apoptotically, (65), while apoptotic death is believed to favor tumor destruction, (66). Indeed, on the one hand apoptotic cells may be captured by specific macrophages called *"tingible body macrophages"*, hence possibly preventing toxic necrosis. On the other hand, apoptosis can lead to an immune response against tumor cells through the activation of T-cells and the perforin-granzyme cellular death pathway, (67, 68), making it possible to foresee tumoral

death at a certain distance from the treated zone, a very interesting mechanism if one wishes to target metastases or infiltrating tumors, which can't be all covered with nanoparticles. Finally, the proliferation of tumor cells has been associated with the loss by these cells of the faculty to die through apoptosis, a behavior that may come from the presence in these cells of an excess of anti-apoptotic proteins such as BH3 or a lack of pro-apoptotic proteins such as BAX, (65,69). Fifthly, it was suggested that exposing magnetosomes to an AMF can trigger the migration of polynuclear neutrophil immune cells (PNN) towards the magnetosome region, *i.e.* PNN are observed in this region persistently 3 and 72 hours following magnetosome injection and 1 to 3 AMF applications. While a direct link between the presence of PNN in the tumor and anti-tumor activity was not established, it was shown that exposing magnetosomes to an AMF could trigger a response of the immune system repetitively by applying the magnetic field several times. For other types of cancer immunotherapies, it was also shown that such response could under certain specific conditions help to destroy the tumor, (70).

One of the most interesting aspects of these studies lies in the faculty of bio-synthesized IONP to modulate anti-tumor activity through multiple applications of the alternating magnetic field, and when this is not sufficient to prevent tumor re-growth through a second nanoparticle administration. Hence, this method enables obtaining efficient anti-tumor activity by using two different parameters to control anti-tumor activity, *i.e.* on the one hand the quantity of active principle (bio-synthesized IONP) in the tumor, and on the other hand the level of activity of this active principle that is determined by the parameters of the external source of energy (AMF), which is applied.

CONCLUSION

In this article, I have presented methods of synthesis of iron oxide nanoparticles by various living organisms such as bacteria, plants, animals or certain by-products of these organisms. This type of fabrication presents the advantage of not relying on the use of toxic chemicals. These nanoparticles have been reported to be composed of various types of iron oxides. Among them, maghemite seems to be the purest and most stable one. Most studies highlight the presence of an organic layer at the surface of these nanoparticles, which is believed to strengthen their biocompatibility. However, for biotechnological applications, it is most probable that it is necessary to remove this layer, since it could be difficult to characterize it fully and to obtain it identically in a reproducible manner from one batch to the other. In addition this layer may contain some allergens. I deduced from my bibliographic search that a NP fabrication process compatible with NP biotechnological needs was only developed for magnetosomes, which are iron oxide nanoparticles synthesized by magnetotactic bacteria, This process enables purifying magnetosomes to remove most organic materials and only keep their non-organic iron oxide mineral part, which is then stabilized by a synthetic coating. Furthermore, it yields NP with favorable properties for biotechnological applications such as: i) a composition in maghemite that is pure and stable, ii) a surface charge that can be adjusted by using various coatings, iii) a current production yield of ~10 mg of magnetosomes per liter of growth medium that is sufficient for the foreseen tumor treatment, iv) a sufficient stability in suspension to enable the administration of these NP at the desired concentration (up to typically 100 mg of magnetosomes per mL of water), v) NP that do not degrade during a few months, vi) NP that disperse homogenously and do not aggregate due to their chain arrangement. Whereas bio-synthesized IONP have been described as being bio-compatible and as being able to induce cytotoxicity towards tumor cells under certain conditions, a detailed evaluation of the anti-tumor activity that such NP could trigger has only been carried out (to the author knowledge) for the magnetosomes, by notably showing that it was possible to fully eradicate certain types of GBM tumors in mice such as intracranial human U87-Luc GBM or subcutaneous GL-261 GBM, by administering magnetosomes in these tumors and by exposing these mice to several sessions of application of an AMF during which the tumor

temperature only moderately increased at typically 41-43 °C. In addition of being efficient, it was shown that this treatment did not induce any observable side effects, possibly due to the moderate heating temperatures reached during treatment and to magnetosome bio-compatibility.

DECLARATION OF INTEREST: Edouard Alphandéry has been working in the company Nanobacterie.

ACKNOWLEDGMENT: We would like to thank the BPI (*''banque publique d'investissement, France''*), the region of Paris (*''Paris Région Entreprise, France''*), the French Research Tax Credit program (*''crédit d'impôt recherche''*), the incubator Paris Biotech Santé, the ANRT (CIFRE 2014/0359, CIFRE 2016/0747, CIFRE 2013/0364, CIFRE 2015/976), the Eurostars programs (Nanoneck-2 E9309 and Nanoglioma E11778), the AIR program (*''aide à l'innovation responsable''*) from the region of Paris (A1401025Q), the ANR (*''Agence Nationale de la Recherche''*) Méfisto, as well as the Universities Paris 6 and Paris 11. We also would like to thank the Nomis Foundation and Markus Reinhard for their support.

FIGURES:

Figure 1: (a), A TEM image of a typical whole MSR-1 magnetotactic bacterium that produces magnetosomes used for the treatments. (b), (c) Two TEM images at different scale of non-pyrogenic magnetosome minerals coated with poly-L-lysine (M-PLL) that display an organization in chains as observed in Figure 1(b) for CM. (d), For a typical mouse treated by administration of 500-700 µg/mm^3 of M-PLL in intracranial U87-Luc tumors of 2 mm^3 followed by 27 magnetic sessions (27 MS), a schematic illustration of the treatment showing: i) M-PLL intra-tumor administration, ii) tumor BLI during the day of M-PLL administration, iii) a typical magnetic session during which the mouse is positioned inside the coil generating the AMF and leading to tumor temperature increases detected by infra-red thermometry, iv) the disappearance of tumor BLI after 27 magnetic sessions. (e), For a typical mouse treated by administration of 25 µg/mm^3 of M-PLL in subcutaneous GL-261 tumors of ~100 mm^3 followed by 15 magnetic sessions (15 MS), a schematic illustration of the treatment showing: i) M-PLL intra-tumor administration, ii) a typical magnetic session during which the mouse is positioned inside the coil generating the AMF and leading to tumor temperature increases detected by infra-red thermometry, iii) the disappearance of the subcutaneous tumor after 15 magnetic sessions.

Figure 2: A schematic diagram presenting the different mechanisms that can trigger anti-tumor activity when magnetosomes are administered in a tumor and further exposed to an alternating magnetic field to induce localized heat. They can be due to magnetosome high SAR values, magnetosome internalization in tumor cells, the apoptotic cell death that magnetosomes can activate, the immune response induced by magnetosomes, closed packed magnetosome distribution that can yield magnetosome bio-persistence in the tumor.

TABLES:

Table 1: For various bio-synthesized IONP, composition, organic part, size, shape, crystallinity, zeta potential, synthesis method, as well as *in vitro* and *in vivo* anti-cancer activities.

Table 2: A summary of the different treatment parameters, indicating: i) the type of nanoparticles administered in the tumor (MC, M-PLL or BNF), ii) the type of treated tumor, *i.e.* either intracranial human U87-Luc GBM tumors of 2-4 mm^3 grown inside the brain of nude mice or subcutaneous murine GL-261 GBM tumors of 100 mm^3 grown subcutaneously under the skin of immune-competent mice, iii) quantities of magnetosomes administered in the tumors, which are comprised between 13 and 700 µg of nanoparticles depending on nanoparticle/protocol type, iv) the strength/frequency of the applied AMF, which are 11-31 mT and 198-202 kHz, respectively, v) the number of magnetic sessions, which is comprised between 11 and 27, vi) the length of each magnetic session that is fixed at 30 minutes, and vii) the percentages of mice with full tumor disappearance that reflects treatment efficacy and is comprised between 0 and 100% depending on treatment conditions.

Table 3: The values of the temperature increases (ΔT) obtained during the various treatments presented whose parameters are given in table 1. || indicates the second injection of the nanoparticles. 1 inject and 2 inject designate protocols with one and two nanoparticle injection(s), respectively. MS1 to MS27 designate the first to the twentieth seventh magnetic session.

Table 4: Heating parameters of the experiment in which 100 mm^3 GL-261 subcutaneous GBM tumors were injected with 25-50 µg of M-PLL per mm^3 of tumor, indicating the magnetic field strength used to reach the indicated maximum temperatures during the first magnetic session, *i.e.* magnetic field strengths of 19±4 mT and 27±4 mT to reach 45-51 °C and 44-47 °C with M-PLL and BNF, respectively, as well as the number of re-injected mice and average magnetic field strength applied during the various sessions for the protocols using M-PLL and BNF.

REFERENCES:

1. Li Y, Q Y, Zhang H, Xia Z, Xie T , Li W, Zhong D, Zhu H, Zhou M. Gram-scale synthesis of highly biocompatible and intravenous injectable hafnium oxide nanocrystal with enhanced radiotherapy efficacy for cancer theranostic, Biomaterials, 2020; 226: 119538.

2. Alphandéry E, Biodistribution and targeting properties of iron oxide nanoparticles for treatments of cancer and iron anemia disease, Nanotoxicology 2019; 13: 573–596.

3. Maier-Hauff K, Rothe R, Scholz R, Gneveckow U, Wust P, Thiesen B, Feussner A, Von Deimling A, Waldoefner N, Felix R, Jordan A, Intracranial thermotherapy using magnetic nanoparticles combined with external beam radiotherapy: Results of a feasibility study on patients with glioblastoma multiforme, J. Neurooncol. 2007; 81: 53-60.

4. Maier-Hauff K, Ulrich F, Nestler D, Niehoff H, Wust P, Thiesen B, Orawa H, Budach V, Jordan A, Efficacy and safety of intratumoral thermotherapy using magnetic iron-oxide nanoparticles combined with external beam radiotherapy on patients with recurrent glioblastoma multiforme, J Neurooncol. 2011; 103: 317-324.

5. Nagajyothi PC, Pandurangan M, Sreekanth TVM, Shim J, In vitro anticancer potential of BaCO3 nanoparticles synthesized via green route, Journal of Photochemistry & Photobiology, B: Biology 2016; 156: 29–34.

6. Ovais M, Khalil AT, Ayaz M, Ahmad I, Nethi SK, Mukherjee S, Biosynthesis of Metal Nanoparticles via Microbial Enzymes: A Mechanistic Approach, *Int. J. Mol. Sci.* 2018; 19: 4100.

7. Siddiqi KS, Rahman AU, Husen TA, Biogenic Fabrication of Iron/Iron Oxide Nanoparticles and Their Application, *Nanoscale Research Letters* 2016; 11: 498.

8. Moghaddam AB, Namvar F, Moniri M, Tahir PM, Azizi S, Mohamad R, Nanoparticles Biosynthesized by Fungi and Yeast: A Review of Their Preparation, Properties, and Medical Applications, *Molecules* 2015; 20: 16540-16565.

9. El-Kassas HY, Aly-Eldeen MA, Gharib SM, Green synthesis of iron oxide (Fe_3O_4) nanoparticles using two selected brown seaweeds: Characterization and application for lead bioremediation, *Acta Oceanol. Sin.* 2016; DOI: 10.1007/s13131-016-0880-3

10. Khandel P, Shahi SK, Mycogenic nanoparticles and their bio-prospective applications: current status and future challenges, Journal of Nanostructure in Chemistry 2018; 8: 369–391.

11. Prozorov T, Mallapragada SK, Narasimhan B, Wang L, Palo P, Nilsen-Hamilton M, Williams TJ, Bazylinski DA, Prozorov R, Canfield PC, Protein-Mediated Synthesis of Uniform Superparamagnetic Magnetite Nanocrystals, *Adv. Funct. Mater*. 2007; 17: 951–957.

12. Shipunova VO, Kotelnikova PA, Aghayeva UF, Stremovskiy OA, Novikov IA, Schulga AA, Nikitin MP, Deyev SM, Self-assembling nanoparticles biofunctionalized with magnetite-binding protein for the targeted delivery to HER2/neu overexpressing cancer cells, *Journal of Magnetism and Magnetic Materials* 2019; 469: 450–455.

13. Tanaka M, Mazuyama E, Arakaki A, Matsunaga T, MMS6 Protein Regulates Crystal Morphology during Nano-sized Magnetite Biomineralization in Vivo, *The journal of biological chemistry* 2011; 286: 6386–6392.

14. Valverde-Tercedor C, Montalbán-López M, Perez-Gonzalez T, Sanchez-Quesada MS, Prozorov T, Pineda-Molina E, Fernandez-Vivas MA, Rodriguez-Navarro AB, Trubitsyn D, Bazylinski DA, Jimenez-Lopez C, Size control of in vitro synthesized magnetite crystals by the MamC protein of Magnetococcus marinus strain MC-1, *Applied Microbiology and Biotechnology* 2015; 99: 5109–5121.

15. Berny C, Le Fèvre R, Guyot F, Blondeau K, Guizonne C, Rousseau E, Bayan N, Alphandéry E, A Method for Producing Highly Pure Magnetosomes in Large Quantity for Medical Applications Using

Magnetospirillum gryphiswaldense MSR-1 Magnetotactic Bacteria Amplified in Minimal Growth Media, Frontiers in Bioengineering and Biotechnology, 2020; 8: 16.

16. Alphandéry E, Ngo AT, Lefèvre C, Lisiecki I, Wu LF, Pileni MP, Difference between the Magnetic Properties of the Magnetotactic Bacteria and Those of the Extracted Magnetosomes: Influence of the Distance between the Chains of Magnetosomes, J. Phys. Chem. C 2008; 112: 12304–12309.

17. Mandawala C, Chebbi I, Durand-Dubief M, Le Fèvre R, Hamdous Y, Guyot F, Alphandéry E, Biocompatible and stable magnetosome minerals coated 1 with poly-L-lysine, citric acid, oleic acid, and carboxy-2 methyl-dextran, for application in the magnetic 3 hyperthermia treatment of tumors, J. Mater. Chem. B, 2017; 5: 7644-7660.

18. Hamdous Y, Chebbi I, Mandawala C, Le Fèvre R, Guyot F, Seksek O, Alphandéry E, Biocompatible coated magnetosome minerals with various organization and cellular interaction properties induce cytotoxicity towards RG-2 and GL-261 glioma cells in the presence of an alternating magnetic field, J. Nanobiotechnoly, 2017; 15: 74.

19. Alphandéry E, Idbaih A, Adam C, Delattre JY, Schmitt C, Guyot F, Chebbi I, Alphandéry E, Chains of magnetosomes with controlled endotoxin release and partial tumor occupation induce full destruction of intracranial U87-Luc glioma in mice under the application of an alternating magnetic field, Journal of Controlled Release, 2017a, 262: 259-272.

20. Alphandéry E, Idbaih A, Adam C, Delattre JY, Schmitt C, Guyot F, Chebbi I, Development of non-pyrogenic magnetosome minerals coated with poly-l-lysine leading to full disappearance of intracranial U87-Luc glioblastoma in 100% of treated mice using magnetic hyperthermia, Biomaterials, 2017b, 141, 210.

21. Le Fèvre R, Durand-Dubief M, Chebbi I, Mandawala C, Lagroix F, Valet JP, Idbaih A, Adam C, Delattre JY, Schmitt C, Maake C, Guyot F, Alphandéry E, Enhanced antitumor efficacy of

biocompatible magnetosomes for the magnetic hyperthermia treatment of glioblastoma, Theranostics, 2017; 7: 4618-4631.

22. Bazylinski DA, Frankel R, Magnetosome formation in prokaryotes, Nature Reviews in Microbiology 2004; 2: 217-230.

23. Byrne JM, Muhamadali H, Coker VS, Cooper J, Lloyd JR, Scale-up of the production of highly reactive biogenic magnetite nanoparticles using Geobacter sulfurreducens, J. R. Soc. Interface, 2015; 12: 20150240.

24. Fatemi M, Mollania N, Momeni-Moghaddam M, Sadeghifar F, Extracellular biosynthesis of magnetic iron oxide nanoparticles by Bacillus cereus strain HMH1: Characterization and in vitro cytotoxicity analysis on MCF-7 and 3T3 cell lines, Journal of Biotechnology, 2018; 270: 1–11.

25. Jacob PJ, Masarudin MJ, Hussein MZ, Rahim RA, Facile aerobic construction of iron based ferromagnetic nanostructures by a novel microbial nanofactory isolated from tropical freshwater wetlands, Microb Cell Fact, 2017; 16: 175.

26. Kianpour S, Ebrahiminezhad A, Mohkam M, Tamaddon AM, Dehshahri A, Heidari R, Ghasemi Y, Physicochemical and biological characteristics of the nanostructured polysaccharide-iron hydrogel produced by microorganism Klebsiella oxytoca, J. Basic Microbiol, 2017; 57: 132–140.

27. Kianpour S, Ebrahiminezhad A, Deyhimi M, Negahdaripour M, Raee MJ, Mohkam M, Rezaee H, Irajie C, Berenjian A, Ghasemi Y, Structural characterization of polysaccharide-coated iron oxide nanoparticles produced by Staphylococcus warneri, isolated from a thermal spring, J Basic Microbiol, 2019; 59: 569-578.

28. Bereczk-Tompa E, Vonderviszt F, Horváth B, Szalaid I, Pósfai M, Biotemplated synthesis of magnetic filaments, Nanoscale 2017; 9: 15062-15069.

29. Alam T, Khan RAA, Ali A, Sher H, Ullah Z, Ali M, Biogenic synthesis of iron oxide nanoparticles via Skimmia laureola and their antibacterial efficacy against bacterial wilt pathogen Ralstonia solanacearum, Materials Science & Engineering C 2019; 98: 101–108.

30. Devi HS, Boda MA, Shah MA, Parveen S, Wani AH, Green synthesis of iron oxide nanoparticles using Platanus orientalis leaf extract for antifungal activity, Green Process Synth 2019; 8: 38–45.

31. Farshchi HK, Azizi M, Jaafari MR, Nemati SH, Fotovat A, Green synthesis of iron nanoparticles by Rosemary extract and cytotoxicity effect evaluation on cancer cell lines, Biocatalysis and Agricultural Biotechnology, 2018; 16: 54–62.

32. Martínez-Cabanas M, López-García M, Barriada JL, Herrero R, Sastre de Vicente ME, Green synthesis of iron oxide nanoparticles. Development of magnetic hybrid materials for efficient As(V) removal, Chemical Engineering Journal, 2016; 301: 83–91.

33. Moniri M, Boroumand A, Azizi MS, Rahim RA, Saad WZ, Navaderi M, Arulselvan P, Mohamad R, Molecular study of wound healing after using biosynthesized BNC/Fe3O4 nanocomposites assisted with a bioinformatics approach, International Journal of Nanomedicine, 2018; 13: 2955–2971.

34. Pallela PNVK, Ummey S, Ruddaraju LK, Gadi S, Cherukuri CS, Barla S, Pammi SVN, Antibacterial efficacy of green synthesized α-Fe2O3 nanoparticles using Sida cordifolia plant extract, Heliyon, 2019; 5: e02765.

35. Plachtová P, Medříková Z, Zbořil R, Tuček J, Varma RS, Maršálek B, Iron and Iron Oxide Nanoparticles Synthesized Using Green Tea Extract: Improved Ecotoxicological Profile and Ability to Degrade Malachite Green, ACS Sustain Chem Eng. 2018; 6: 8679–8687.

36. Prasad AS, Iron oxide nanoparticles synthesized by controlled bio-precipitation using leaf extract of Garlic Vine (Mansoa alliacea), Materials Science in Semiconductor Processing 2016; 53: 79–83.

37. Nazeer AA, Udhayakumar S, Mani S, Dhanapal M, Vijaykumar SD, Surface modification of Fe2O3 and MgO nanoparticles with agrowastes for the treatment of chlorosis in Glycine max, Nano Convergence 2018; 5: 23.

38. Deshmukh AR, Gupta A, Kim BS, Ultrasound Assisted Green Synthesis of Silver and Iron Oxide Nanoparticles Using Fenugreek Seed Extract and Their Enhanced Antibacterial and Antioxidant Activities, BioMed Research International, Volume 2019, Article ID 1714358.

39. Nagajyothi PC, Pandurangan M, Kim DH, Sreekanth TVM, Shim J, Green Synthesis of Iron Oxide Nanoparticles and Their Catalytic and In Vitro Anticancer Activities, J. Clust. Sci. 2016; 28: 245-257.

40. Moshafi MH, Ranjbar M, Ilbeigi G, Biotemplate of albumen for synthesized iron oxide quantum dots nanoparticles (QDNPs) and investigation of antibacterial effect against pathogenic microbial strains, International Journal of Nanomedicine, 2019; 14: 3273–3282.

41. Li X, Wang C, Zeng Y, Li P, Xie T, Zhang Y. Bacteria-assisted preparation of nano Fe2O3 red pigment powders from waste ferrous sulfate, Journal of Hazardous Materials, 2016; 317: 563–569

42. Bain J, Legge CJ, Beattie DL, Sahota A, Dirks C, Lovett JR, Staniland SS, A biomimetic magnetosome: formation of iron oxide within carboxylic acid terminated polymersomes, Nanoscale, 2019; 11: 11617-11625.

43. Rawlings AE, Somner LA, Fitzpatrick-Milton M, Roebuck TP, Gwyn C, Liravi P, Seville V, Neal TJ, Mykhaylyk OO, Baldwin SA, Staniland SS, Artificial coiled coil biomineralisation protein for the synthesis of magnetic nanoparticles, Nature communications, 2019; 10: 2873.

44. Liu L, Pu X, Yin G, Chen X, Yin J, Wu Y, Biomimetic Mineralization of Magnetic Iron Oxide Nanoparticles Mediated by Bi-Functional Copolypeptides, Molecules, 2019; 24: 1401.

611 45. Alphandéry E, Ngo AT, Lefèvre C, Lisiecki I, Wu LF, Pileni MP, Difference between the Magnetic
612 Properties of the Magnetotactic Bacteria and Those of the Extracted Magnetosomes: Influence of
613 the Distance between the Chains of Magnetosomes, *J. Phys. Chem. C* 2008; 112: 12304-12309

614 46. Schweiger C, Hartmann R, Zhang F, Parak WJ, Kissel TH, Rivera_Gil P, Quantification of the
615 internalization patterns of superparamagnetic iron oxide nanoparticles with opposite charge, Journal
616 of Nanobiotechnology, 2012; 10: 28.

617 47. Forest V, Pourchez J, Preferential binding of positive nanoparticles on cell membranes is due to
618 electrostatic interactions: A too simplistic explanation that does not take into account the
619 nanoparticle protein corona, Mater Sci Eng C Mater Biol, 2017; 70: 889-896.

620 48. Ayala V, Herrera AP, Latorre-Esteves M, Torres-Lugo M, Rinaldi C, Effect of surface charge on
621 the colloidal stability and in vitro uptake of carboxymethyl dextran-coated iron oxide nanoparticles,
622 J Nanopart Res., 2013; 15: 1874-1898.

623 49. Alphandéry E, Faure S, Seksek O, Guyot F, Chebbi I. Chains of Magnetosomes Extracted from
624 AMB-1 Magnetotactic Bacteria for Application in Alternative Magnetic Field Cancer Therapy,
625 ACSnano 2011; 5: 6279-6296.

626 50. Sulaiman GM, Tawfeeq AT, Naji AS, Biosynthesis, characterization of magnetic iron oxide
627 nanoparticles and evaluations of the cytotoxicity and DNA damage of human breast carcinoma cell
628 lines, Artificial Cells, Nanomedicine, and Biotechnology, 2018; 46: 1215–1229.

629 51. Gahlawat G, Choudhury AR, A review on the biosynthesis of metal and metal salt nanoparticles by
630 microbes, RSC Adv., 2019; 9: 12944-12967.

631 52. Safaepour M, Shahverdi AR, Shahverdi HR, Khorramizadeh MR, Gohari AR, Green synthesis of
632 small silver nanoparticles using geraniol and its cytotoxicity against fibrosarcoma-wehi 164.
633 Avicenna J Med Biotechnol, 2009; 1:111–115.

53. D'Britto V, Devi PP, Prasad BLV, Dhawan Mantri VG, Prabhune A, Medicinal plant extracts used for blood sugar and obesity therapy shows excellent inhibition of invertase activity: synthesis of nanoparticles using this extract and its cytotoxic and genotoxic effects. Int J life Sci Pharma Res, 2012; 2: 61–74.

54. Nazeer AA, Udhayakumar S, Mani S, Dhanapal M, Vijaykumar SD, Surface modification of Fe2O3 and MgO nanoparticles with agrowastes for the treatment of chlorosis in Glycine max, Nano Convergence, 2018; 5: 23.

55. Dorniani D, Hussein MZB, Kura AU, Fakurazi S, Shaari AH, Ahmad Z, Preparation of Fe3O4 magnetic nanoparticles coated with gallic acid for drug delivery, International Journal of Nanomedicine, 2012; 7: 5745–5756.

56. Gholami L, Oskuee RK, Tafaghodi M, Farkhani AR, Darroudi M, Green facile synthesis of low-toxic superparamagnetic iron oxide nanoparticles (SPIONs) and their cytotoxicity effects toward Neuro2A and HUVEC cell lines, Ceramics International, 2018; 44: 9263–9268.

57. Majid Darroudid Khalil AT, Ovais M, Ullah I, Ali M, Shinwari ZK, Maaza M, Biosynthesis of iron oxide (Fe2O3) nanoparticles via aqueous extracts of Sageretia thea (Osbeck.) and their pharmacognostic properties, Green chemistry letters and reviews, 2017; 10: 186–201.

58. Hafiz SM, Kulkarni SS, Thakur MK, In-vivo Toxicity Assessment of Biologically Synthesized Iron Oxide Nanoparticles in Zebrafish (Danio rerio), Biosciences biotechnology research asia, 2018, 15: 419-425.

59. Markova Z, Novak P, Kaslik J, Plachtova P, Brazdova M, Jancula D, Siskova KM, Machala L, Marsalek B, Zboril R, Varma R, Iron(II,III)−Polyphenol Complex Nanoparticles Derived from Green Tea with Remarkable Ecotoxicological Impact, ACS Sustainable Chem. Eng. 2014; 2: 1674−1680.

60. Lakshmi PP, Krishna MG. Venkateswara RK, Shanker K, Biosynthesis, characterization and acute oral toxicity studies of synthesized iron oxide nanoparticles using ethanolic extract of Centella asiatica plant, Materials Letters, 2019, 236: 256–259.

61. Njagi EC, Huang H, Stafford L, Genuino H, Galindo HM, Collins JB, Hoag GE, Suib SL, Biosynthesis of Iron and Silver Nanoparticles at Room Temperature Using Aqueous Sorghum Bran Extracts, Langmuir, 2011, 27: 264–271.

62. Namvar F, Rahman HS, Mohamad R, Baharara J, Mahdavi M, Amini E, Chartrand MS, Yeap SK, Cytotoxic effect of magnetic iron oxide nanoparticles synthesized via seaweed aqueous extract, International Journal of Nanomedicine, 2014; 9: 2479–2488.

63. Izadiyan Z, Shameli K, Miyake M, Hara H, Mohamad SEB, Kalantari K, Taib SHM, Rasouli E, Cytotoxicity assay of plant-mediated synthesized iron oxide nanoparticles using Juglans regia green husk extract, *Arabian Journal of Chemistry*, 2020; 13: 2011–2023.

64. Alphandéry E, Faure S, Raison L, Duguet E, Howse PA, Bazylinski D, Heat Production by Bacterial Magnetosomes Exposed to an Oscillating Magnetic Field, J. Phys. Chem. C, 2011; 115: 18–22.

65. Warren CFA, Wong-Brown MW, Bowden NA, BCL-2 family isoforms in apoptosis and cancer, Cell Death and Disease, 2019; 10: 177.

66. Wong RSY, Apoptosis in cancer: from pathogenesis to treatment, Journal of Experimental & Clinical Cancer Research, 2011; 30: 87.

67. Voskoboinik I, Whisstock JC, Trapani JA, Perforin and granzymes: function, dysfunction and human pathology, Nature reviews immunology, 2015; 15: 388-400.

68. Kale J, Osterlund EJ, Andrews DW, BCL-2 family proteins: changing partners in the dance towards death, Cell Death and Differentiation, 2018; 25: 65–80.

69. Cook KW, Durrant LG, Brentville VA, Current Strategies to Enhance Anti-Tumour Immunity, Biomedicines, 2018; 6: 37.

70. Oberg HH, Wesch D, Kalyan S, Kabelitz D, Regulatory Interactions Between Neutrophils, Tumor Cells and T Cells, Frontiers in Immunology, 2019; 10: 1690.

71. Ahmed A, Abagana A, Cui D, Zhao M, De Novo Iron Oxide Hydroxide, Ferrihydrite Produced by Comamonas testosteroni Exhibiting Intrinsic Peroxidase-Like Activity and Their Analytical Applications, BioMed Research International, Volume 2019, Article ID 7127869.

72. Chariaou M, Rahn-Lee L, Kind J, Garcıa-Rubio I, Komeili A, Gehring AU, Anisotropy of Bullet-Shaped Magnetite Nanoparticles in the Magnetotactic Bacteria Desulfovibrio magneticus sp. Strain RS-1, Biophysical Journal Volume, 2015; 108: 1268–1274.

73. Martínez-Cabanas M, López-García M, Barriada JL, Herrero R, Vicente MESD, Green synthesis of iron oxide nanoparticles. Development of magnetic hybrid materials for efficient As(V) removal, Chemical Engineering Journal, 2016; 301: 83–91.

74. Xiao Z, Yuan M, Yang B, Liu Z, Huang J, Sun D, Plant-mediated synthesis of highly active iron nanoparticles for Cr (VI) removal: Investigation of the leading biomolecules, Chemosphere, 2016, 150: 357-364.

75. Yan Q, Street J, Yu F, Synthesis of carbon-encapsulated iron nanoparticles from wood derived sugars by hydrothermal carbonization (HTC) and their application to convert bio-syngas into liquid hydrocarbons, Biomass and Bioenergy 2015, 83: 85-95.

76. Sharan C, Khandelwal P, Poddar P, The mechanistic insight into the biomilling of goethite (a-FeO(OH)) nanorods using the yeast Saccharomyces cerevisiae, RSC Adv., 2015, 5: 91785-91794.

77. Subramaniyam V, Subashchandrabose SR, Thavamani P, Megharaj M, Chen Z, Naidu R, Chlorococcum sp. MM11—a novel phyco-nanofactory for the synthesis of iron nanoparticles, J Appl Phycol, 2015, DOI 10.1007/s10811-014-0492-2.

78. Truskewycz A, Shukla R, Ball AS, Phytofabrication of Iron Nanoparticles for Hexavalent Chromium Remediation, ACS Omega, 2018, 3: 10781−10790.

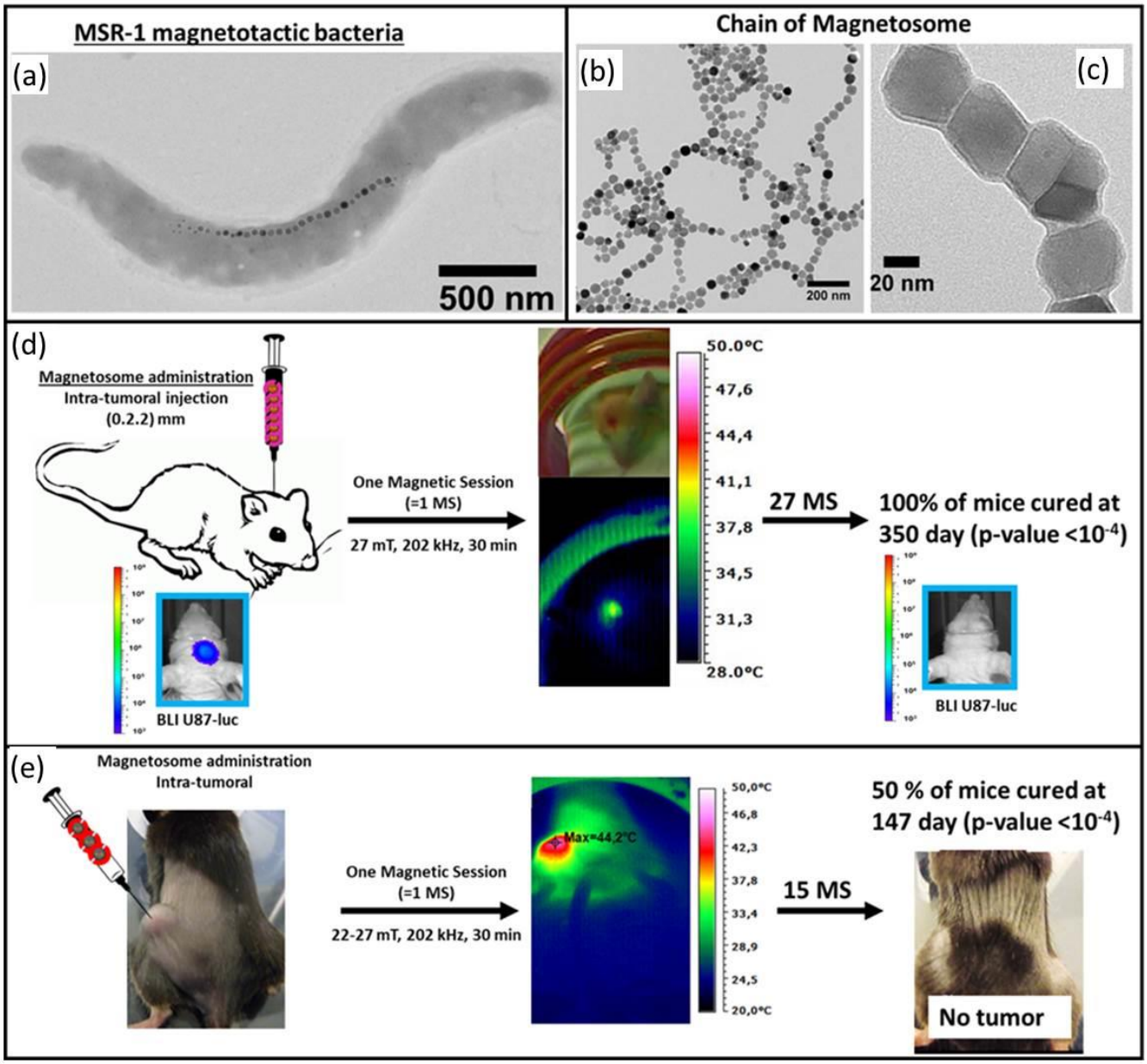
MSR-1 magnetotactic bacteria
(a)
500 nm
Chain of Magnetosome
(b)
200 nm
(c)
20 nm
(d)
Magnetosome administration
Intra-tumoral injection
(0.2.2) mm
BLI U87-luc
One Magnetic Session
(=1 MS)
27 mT, 202 kHz, 30 min
50.0°C
47,6
44,4
41,1
37,8
34,5
31,3
28.0°C
27 MS
100% of mice cured at
350 day (p-value <10-4)
BLI U87-luc
(e)
Magnetosome administration
Intra-tumoral
One Magnetic Session
(=1 MS)
22-27 mT, 202 kHz, 30 min
Max=44.2°C
50,0°C
46,8
42,3
37,8
33,4
28,9
24,5
20,0°C
15 MS
50 % of mice cured at
147 day (p-value <10-4)
No tumor

Figure 1

707

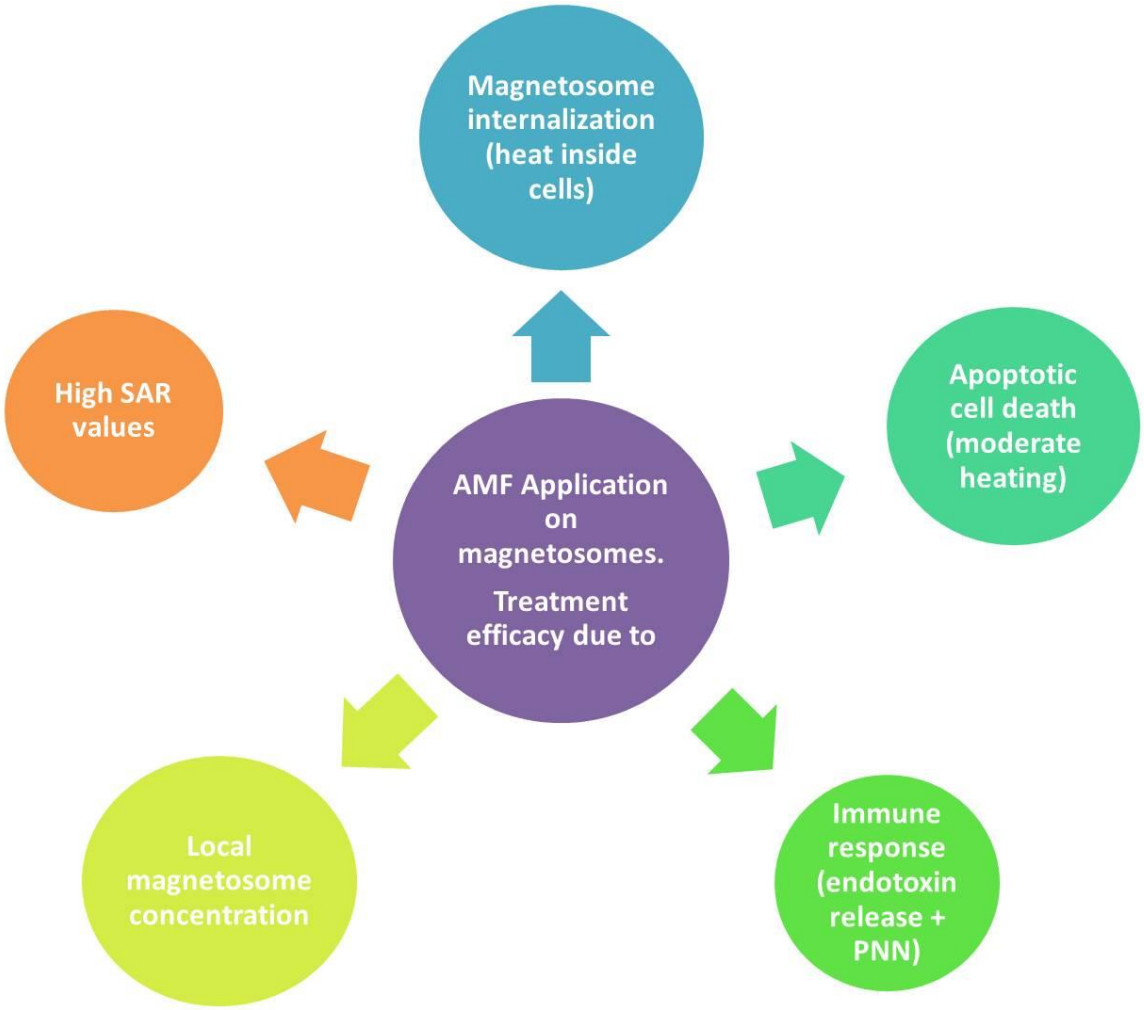

Figure 2

708

709

Metal. Comp.	Organic part	Size Shape Crystallinity Zeta potential	Synthesis	Efficacy results (*in vitro* & *in vivo*)	Ref
NP FeO(OH) Ferrihydrite Superparamagnetic	NP inside cytoplasmic membrane	80 nm Spherical Crystalline	NP produced by bacterial strain recognized as Comammonas testosteroni	NA	Ahmed2019, 71
NP Fe_2O_3 (no exact composition given)	NP capped by biomolecules (Skimmidiol)	56-350 nm Cubic Crystalline	NP synthesized in the presence of *Skimmia laureola leaf extract*	NA	Alam2019, 29
NP magnetite	polymersome	250 nm (aggregation of 5 nm NP)	Polymersome made of copolymers PEG113-PHPMA400 and PMPC28-PHPMA400 used to synthesized NP	NA	Bain2019, 42
NP Magnetite	organic material of flagella	1.5-15 nm Crystalline (chains along filament)	co-precipitation of Fe(II) and Fe(III) in the presence of mutant *Salmonella* bacteria.	NA	Bereczk2017, 28
NP mixed composition: magnetite + goethite + haematite + siderite	NA	10-15 nm Crystalline Sphere	NP synthesized by *G. sulfurreducens* bacteria	NA	Byrne2015, 23
NP Magnetite	NA	40-60 nm Crystalline	*NP synthesized by Desulfovibrio magneticus sp. Strain RS-1* magnetotactic bacteria	NA	Chariaou2015, 72
NP (Superparmagnetic)	fenugreek seed phytochemicals	20 nm (W US) 35 nm (WO US) Crystalline Sphere	Coprecipitation: *Fenugreek Seed* Extract mixed with $FeCl_2$ + $FeCl_3$.	NA	Deshmukh2019, 38
NP mixed composition: α-Fe2O3 and γ-Fe2O3)	Coating: organic components of *Platanus orientalis* leaf extract	40 nm (TEM) 78–80 nm (DLS) Sphere Crystalline	Polyphenols contained in *Platanus orientalis* leaf extract reduces iron ions to form NPs	NA	Devi2019, 30
NP mixed composition: magnetite, maghemite, iron hydroxides	organic materials adsorbed from rosemary extract as a capping/stabilizing agents.	20-80 nm Sphere Amorphous ZP = -19 mV	Leaves of Rosemary extract reduces $FeSO_4$ to NP	IC_{50} of Rosemary-FeNPs and Rosemary alone towards 4T1 breast cancer cells: 44 µg/ml and 100 µg/ml, respectively → higher cytotoxicity of Rosemary-FeNPs than Rosemary alone.	Farshchi2018, 31
NP Magnetite) (Superparamagnetic)	proteins sorption on the nanoparticle surface in the form of capping agents	29 nm Sphere ZP = -11 mV	$FeCl_3$ added to supernatent of bacteria HMH1 strain *Bacillus cereus* Enzymes nitrate reductase reduce metal ions in NP	IC_{50} towards MCF-7 and 3T3 cells are > 5 mg/ml and > 7.5 mg/ml, respectively.	Fatemi2018, 24
NP Magnetite Ferromagnetic (claimed by no hysteresis)	Capping material: Bacterial debris	30-60 nm Sphere Crystalline ZP = 51-60 mV	$FeCl_3$ + $FeSO_4$ mixed with MS2 strain Actinomycetes → extracellular reduction of ferric ions in NP.	NA	Jacob2017, 25
NP Iron hydroxyde (Ferrihydrite) Superparamagnetic	pectin coating	2 nm Sphere Crystalline ZP = -71 mV	polysaccharide-iron hydrogel produced by microorganism *Klebsiella oxytoca*	NA	Kianpour2017, 26
NP Magnetite Superparamagnetic	Polysaccharide/pectin coating	14-77 nm Sphere Crystalline ZP = -91 mV	polysaccharide-coated iron oxide nanoparticles produced by a strain of *Staphylococcus warneri* (from thermal spring)	MTT assay on MOLT-4 cell lines IC_{50} value of 1174 µM (bio-compatibility)	Kianpour2019, 27

Table 1-1

Metal. Comp.	Organic part	Size Shape	Synthesis	Efficacy results (*in vitro & in vivo*)	Ref
NP α-Fe_2O_3 (hematite)	NA	22-86 nm Sphere Crystalline	bacteria-assisted oxidation process by *Acidithiobacillus ferrooxidans* of ferrous sulfate. NP production steps: bio-oxidation, precipitation and calcination.	NA	Li2016, 41
NP Fe_3O_4 (one phase) (Superparamagnetic)	peptide and ginger extract	7 nm (TEM) 55 nm (DLS) Sphere Crystalline (crystallinity decreases with increasing ginger extracts) ZP = -19 mV	Magnetic Iron Oxide Nanoparticles biomineralization by bi-Functional Copolypeptides	NA	Liu2019, 44
NP mixed composition: (maghemite, lepidocrocite, hematite)	NP encapsulated in a chitosan matrix	NA	$Fe(NO_3)$ mixed with eucalyptus extract produces NP which are mixed with a chitosan solution for stabilization.	NA	Martinez-Cabanas2016, 73
Fe_3O_4 NP	NPs coated with biomolecules of *A. vera* extract with antibacterial ability	15-30 nm Crystalline	Magnetic nanoparticles were biosynthesized by using *Aloe vera* extract in new isolated bacterial nanocellulose (BNC) RM1.	The BNC/Fe3O4 was nontoxic towards HDF cells (IC_{50} > 500 µg/mL)	Moniri2018, 33
Iron oxide quantum dots (QD) NP	albumen matrix chains surrounding QD NP	< 80 nm Spherical Crystalline	Iron oxide QD NP prepared using albumen as biotemplate. NP formation → Fe source + egg whites	NA	Moshafi2019, 40
α-Fe_2O_3 (hematite) NP	Organic material coming from plant extract	39 nm Crystalline Sphere	Iron (III) chloride reduced by extract of *Psoralea corylifolia* seeds	NP (0.05-0.4 mg/mL) → cytotoxic towards MDCK cancer cells / not cytotoxic towards healthy Caki-2 cells.	Nagajyothi2016, 5
α-Fe_2O_3 (hematite) NP	proteins	< 30 nm Crystalline	Agrowastes of *Coriandrum sativum* for synthesis of Fe_2O_3 NP functional groups of agro waste extracts reduce metallic salt solution of iron in NP.	Low cytotoxicity of NP on human embryo kidney (HEK-293) cells → more than 50% of cells survive at 500 µg/mL NP.	Nazeer2018, 37
α-Fe_2O_3 (hematite) NP	Coating: *Sida cordifolia* plant extract	20 nm Crystalline Sphere (cluser formation)	Iron nitrate reduced by *Sida cordifolia* plant extract	NA	Pallela2019, 34
Maghemite NP (Superparamagnetic)	Stabilization by green tea extract	< 5 nm (TEM) 215 nm (DLS) amorphous ZP = 11 mV	Iron nitrate mixed with green tea extract	NA	Plachtová2018, 35
β-Fe_2O_3 NP (superparmagnetic suggested)	Stabilized by phenol in leaf extract	15 nm (XRD) Crystalline Sphere	Reduction of hepta hydrous iron sulphate by Garlic Vine leaf extract.	NA	Prasad2016, 36
Magnetite NP M_S (70-90 emu/g)	NA	21-136 nm MPS (TEM) Depending of protein type crystalline	Artificial scaffold proteins added to magnetite co-precipitation reaction.	NA	Rawlings2019, 43

Table 1-2

Metal. Comp.	Organic part	Size Shape	Synthesis	Efficacy results (*in vitro & in vivo*)	Ref
Iron NP	organic materials coated on the Fe NPs	5 nm Spherical amorphous	Ferric chloride ($FeCl_3$) mixed with various plant extracts	NA	Xiao2016, 74
Carbon-encapsulated iron NP	carbon-encapsulation	100-150 nm total 10-25 nm (iron core)	$FeCl_2$ reduced by wood derived sugars followed by carbonization (heating at 110 °C in the presence of calcium carbonate)	NA	Yan2015, 75
goethite (α-FeO(OH)) nanorods transformed in spherical NP	Protein coating	< 10 nm Sphere crystalline	$FeCl_3$ mixed with $FeCl_2$ in HCl → heating at 70 °C with urea → precipitate mixed with Yeast *Saccharomyces cerevisiae*	NA	Sharan2015, 76
Iron NP Yield: 5 µg/L	Capping: carbohydrates and proteinss	20-50 nm (DLS) 20-50 nm (TEM) Sphere Crystalline	iron chloride solution turned into a yellowish brown color when treated with Chlorococcum (both intracellular and extracellular NP)	NA	Subramaniyam2015, 77
Magnetite NP (ferromagnetic claimed by no hysteresis curve)	Capping: plant extract	32-100 nm Sphere Crystalline	Fe^{3+} ions reduced by *Albizia adianthifolia* leaf extracts	IC_{50} of NP on AMJ-13 cells: 1.8 µg/mL IC_{50} of NP on MCF-7 cells: 7.7 µg/mL IC_{50} of plant extracts on AMJ-13 cells > 60 µg/mL IC_{50} of plant extract on MCF-7 cells > 60 µg/mL Antioxidant activity (ROS scavenging): due to functional groups of leaf extracts	Sulaiman2018, 50
NP Mixed composition: Fe_2O_3, FeOOH and/or $Fe(OH)_3$	Capping: phytochemicals	5-100 nm (TEM) Crystalline (agglomeration)	Reduction of iron salts by plant extracts 4 different plants (*Pittosporum undulatum, Melia azedarach, Schinus molle, and Syzygium paniculatum*) NP size depends on plant extract	NA	Truskewycz2018, 78
Magnetosomes intermediate composition maghemite, Magnetite (ferrimagnetic) Yield: 10 mg per liter of growth medium	Iron oxide mineral part surrounded by organic bacterial coating made of lipids/proteins	40 nm (average) Cubo-octahedric Chain arrangment Crystalline ZP = -18 mV (pH 6)	Synthesis by MSR-1 *Gryphiswaldense* magnetotactic bacteria followed by extraction of chains of magnetosomes from these bacteria. → Magnetosomes are pyrogenic	Injection of magnetosomes in glioblastoma followed by several AMF applications leads to full tumor disapperance	Alphandéry 2017, 19
Magnetosoomes intermediate composition maghemite, Magnetite (ferrimagnetic) Yield: 10 mg per liter of growth medium	Iron oxide mineral part surrounded by synthetic coating (PLL)	40 nm (average) Cubo-octahedric Chain arrangment Crystalline Zeta potential positive	Synthesis by MSR-1 *Gryphiswaldense* magnetotactic bacteria followed by extraction of chains of magnetosomes from these bacteria, purification of the chains to remove all organic material surrounding magnetosome mineral core, coating of the core with PLL. → Magnetosomes are non-pyrogenic	Injection of magnetosomes in glioblastoma followed by several AMF applications leads to full tumor disappearance	Alphandéry2017, 20

Table 1-3

metal: Comp.: metallic composition; NP: Nanoparticles; NA: Not available; MPS: Mean particle size; MTB: Magnetotactic bacteria; CA: citric acid; CMD: Carboxy-methyl-dextran; OA: Oleic acid; PEI: Polyethyleneimine; PLL: Poly-L-lysine.

713

Treatment parameters

Treatment number	Nanoparticle type	Tumor type	Tumor size (mm^3)	Mouse type	Quantity administered (µg of nanoparticles per mm^3 of tumor)	AMF strength Frequency	Number of sessions	Lenght of session (min)	Percentage of tumors that have fully disappeared (%)
1	MC	U87-Luc (intracranial)	3-5	Immuno-depressive	13	30 mT 198 kHz	15	30	40
2	BNF	U87-Luc (intracranial)	3-5	Immuno-depressive	13	30 mT 198 kHz	15	30	0
3	M-PLL	U87-Luc (intracranial)	2	Immuno-depressive	500-700	27 mT 202 kHz	27	30	100
4	BNF	U87-Luc (intracranial)	2	Immuno-depressive	500-700	27 mT 202 kHz	23	30	20
5	M-PLL	GL-261 (subcutaneous)	50-150	Immuno-competent	25	11-31 mT 198kHz	15	30	50
6	BNF	GL-261 (subcutaneous)	50-150	Immuno-competent	25	11-31 mT 198kHz	15	30	20

Table 2

714
715

716
717

Heating parameters

Tr N^0	Nano Type	ΔT MS1	ΔT MS2	ΔT MS3	ΔT MS4	ΔT MS5	ΔT MS6	ΔT MS7	ΔT MS8	ΔT MS9	ΔT MS10	ΔT MS11	ΔT MS12	ΔT MS13	ΔT MS14	ΔT MS15	ΔT MS16	ΔT MS17	ΔT MS18	ΔT MS19	ΔT MS20	ΔT MS21	ΔT MS22 to MS27
1	MC	4°C	1.8°C	0.4°C	0.4°C	0°C	0°C	0°C	0°C	0°C	0°C	0°C	0°C	NA	NA	NA	NA	NA	NA	NA	NA	NA	NA
2	BNF	0°C	0°C	0°C	0°C	0°C	0°C	0°C	0°C	0°C	0°C	0°C	0°C	NA	NA	NA	NA	NA	NA	NA	NA	NA	NA
3	M-PLL (1 inject)	18°C	17°C	10°C	7°C	7°C	7°C	7°C	7°C	7°C	7°C	7°C	7°C	7°C	7°C	7°C	2°C	0°C	0°C	0°C	0°C	0°C	0°C
3	M-PLL (2 inject)	18°C	17°C	10°C	7°C	7°C	7°C	7°C	7°C	7°C	7°C	7°C	7°C	7°C	7°C	7°C	2°C	0°C	0°C	‖ 15°C	15°C	15°C	8°C
4	BNF (2 inject)	8°C	0°C	0°C	0°C	0°C	0°C	0°C	0°C	0°C	0°C	0°C	0°C	0°C	0°C	0°C	0°C	0°C	‖ 5°C	0°C	0°C	0°C	0°C

‖ Second injection of nanoparticles

Tr N^0: Treatment number
Nano Type: Type of nanoparticle
1 inject: 1 injection of nanoparticles
2 inject: 2 injections of nanoparticles
ΔT: Temperature variation between the beginning and the end of the magnetic session
MS1-MS27: Magnetic session 1 to magnetic session 27

Table 3

718
719

720

Heating parameters

Treatment number	Nanoparticle type	Magnetic field strength (MS1)	Number of reinjected mice
5	M-PLL	20 ± 7 mT	4
6	BNF	26.5 ± 4.5 mT	6

Table 4

721